CHEMICAL ENGINEERING TRANSACTIONS
VOL. 65, 2018
A publication of AIDIC
The Italian Association of Chemical Engineering
Online at www.aidic.it/cet
Guest Editors: Eliseo Ranzi, Mario Costa

ISBN 978-88-95608-62-4; **ISSN** 2283-9216
DOI: 10.3303/CET1865078

Design of a Fast Energy Storage and Energy Conversion System for Electric Vehicle

Peng Wang

School of Electrical Engineering, Xuchang University, Xuchang 461000, China
Wangpeng461@163.com

In this paper, the author researches on a fast energy storage and energy conversion system for electric vehicle. This paper analyses and studies several main energy storage technologies and expounds the energy storage principle, advantages and disadvantages which also presents the application status quo. This paper introduces the current situation of China's power system and the concept and connotation of smart grid in the future. Based on the background of the development and construction of smart grid in China, the application and development direction of energy storage technology are studied. In this paper, the structure of the battery energy storage system is introduced, and the mathematical model of the battery energy storage system is given. The power control strategy of converter is researched and designed. Combined with the development of wind power in China, the application and effect of battery energy storage system in wind power generation in China are studied and analysed.

1. Introduction

It is well known that the design of the ideal DC-DC converter involves many trade-offs. The increase in power density usually means the increase of overall power consumption, as well as the increase of the temperature of the junction temperature, the shell temperature and the PCB. In the same way, the optimization of DC/DC power for medium current to peak current almost always means sacrificing light load efficiency and vice versa (Yang et al., 2015; Errami et al., 2015). Because of the voltage difference between the instruments, the signal in the interconnected wire will add the pressure difference to the signal, causing a voltage "communication" in the wire. This is one of the reasons that audio signals hear 60 Hz noise (or horizontal interference in video signals). Another problem is the flow of current in the signal cable ground wire. The current will also be introduced into the cable and equipment. Therefore, it is the most basic requirement to ensure that the grounding loop current will not cause the problem of the system in the proper design of the grounding line in the system (Sun and Zhang, 2015).

In another example, the grounding loop is a common problem when multiple audio - visual system components are connected together. The common noise in the audio system is often caused by the grounding loop problem. In addition, the "communication sound" can also be a typical grounding loop problem (of course, depending on the AC power voltage frequency used by the country in the country). Of course, the most common example of the ground loop problem is that the system uses instruments connected to the socket, while the other instrument connects different other grounding receptacles in the room.

The DC/DC converter is a voltage converter that effectively outputs the fixed voltage after the input voltage is changed. The DC/DC converter is divided into three types: the boost type DC/DC converter, the step-down DC/DC converter and the up and down DC/DC converter. Three types of control can be used according to the demand. PWM has high control efficiency and has good output voltage ripple and noise. The PFM control model has the advantages of small power consumption even when it is used for a long time, especially in small load. PFM control is implemented in PWM/PFM conversion small load, and it is automatically converted to PWM control when heavy load is loaded. At present, DC-DC converter is widely used in mobile phone, MP3, digital camera, portable media player and other products. In the classification of circuit types, it belongs to the chopper circuit. Figure 1 show the basic circuits of DC/DC converter (Baloch et al., 2016; Tanvir et al., 2015).

Please cite this article as: Peng Wang , 2018, Design of a fast energy storage and energy conversion system for electric vehicle, Chemical Engineering Transactions, 65, 463-468 DOI: 10.3303/CET1865078

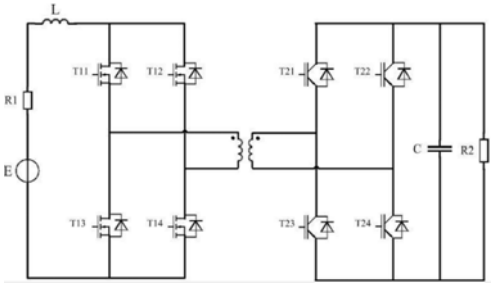

Figure 1: The basic circuits of DC/DC converter

2. The structure of bidirectional power flow circuit for dc/dc converter

The so-called Buck, Boost, Buck Boost and Cuk two-way power conversion circuit, that is, electric energy can flow from the input end to the output terminal, or from the output terminal to the input side, or the input port and the output terminal can be interchanged. To make the PWM DC/DC converter have this function, we must solve the problem of double current flow, and at the same time, when the current is in positive or negative direction, it will not change the equivalent circuit. How to make Buck, Boost, Buck ~ Boost and Cuk PWM DC/DC converter circuit has the function of it, the most simple way is in the original circuit (tube triode switch) on a parallel diode, a transistor in anti-parallel diode on the original circuit (switch), group a two can reverse conducting triode switch S and S. S and S work in a complementary way, that is, when S is turned on, the forward current flows through the original triode and the original diode. When S is turned on, the reverse current can flow through the transistor and diode. This will not only achieve positive and reverse current flow, do not make the equivalent circuit change, Buck, Bcost, Buck will check Boost and Cuk PWM to DC/DC converter circuit as shown in Figure 2, Boost, Buck Boost bidirectional Buck and Cuk PWM DC/DC converter circuit after transforming (Cárdenas et al., 2016).

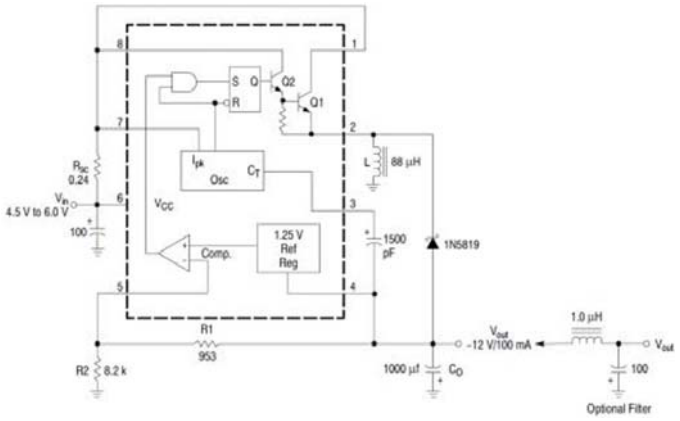

Figure 2: Cuk PWM to DC/DC converter circuit

Reverse bidirectional Buck converter circuit and Boost converter M conversion ratio; reverse bidirectional Boost converter circuit and Buck converter with the same conversion ratio; bidirectional Buck ~ Boost converter and Cuk converter circuit, reverse conversion ratio is the same.

The bidirectional converter circuit is used as the PWM DC/DC converter, and it has good characteristics in practical application. For example, the Cuk bidirectional converter can be used as a current charging converter, when DU=0.5, M=1, M=1, if Ui>U. At the time, the electric energy is Ui to U. Flow; when Ui, <U. At the time, the electric energy is U. Flow to Ui to keep Ui and U_0. Always equal.

Figure 3 shows the power bidirectional Cuk converter circuit and Cuk converter circuit is different: V1 switch (NPN type triode) at both ends of an anti-parallel diode diode DZ; D1 anti parallel a switch (PNP type triode V2). The base of the two switches is connected in parallel, and then the PWM pulse width modulation signal is connected with the current limiting resistance R. The circuit shown in Figure 3, if the right side is a positive and negative voltage source, and the left side is a load resistor, the electric energy will transmit to the left side from the right side, and the output voltage will be positive and negative. On the other hand, if the voltage source is at the left end (up and down negative) and the load resistance is connected to the right end, the electric

energy is transferred from the left end to the right side, and the negative upper voltage is lower positive and negative. The circuit shown in figure 3 will appear a discontinuous conduction mode when the load current is 12 hours. Diode will not flow backward through the current when the diode current drops to zero. But the circuit has a bypass tri - transistor that can lead the reverse current. Therefore, there is no discontinuous working mode in any small load current. This is very beneficial to the stable operation of the circuit. The so-called complementary way of work is in the period of DUTS (DU is duty cycle, Ts is the switching period), the switch S opens, the S turns off; during (1 DU) Ts, the switch s opens, and the S turns off.

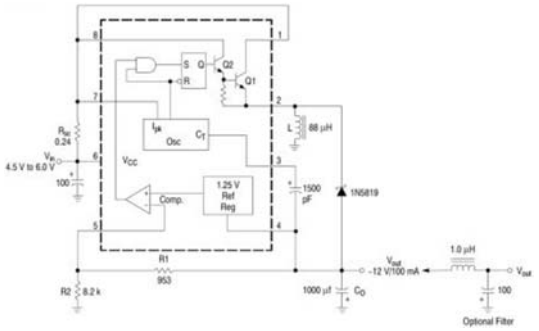

Figure 3: Cuk PWM to DC/DC converter circuit

3. System and algorithm

In order to output the correct voltage value and manage power between different power sources and energy storage units, an efficient DC/DC converter must be used. The DC - DC converter converts a set of voltages and currents to different voltages and currents, and is limited by the maximum power. For example, 12 V turns 400 V (and vice versa), and the maximum power in this case is 1.5 Kw. In this configuration, the battery is maintained for the dashboard actuator and lighting system. The standard voltage is 12V 200-800V, and the DC bus voltage is used to supply the power system.

The technical specifications of bidirectional DC to DC converter are as follows: low voltage terminal nominal input voltage is 12V, during charging and discharging voltage, it may change from 8V to 16V. The nominal input voltage of high voltage terminal is 288V, and the working voltage range varies between 255V-425V. The nominal charge and discharge power is 1.5kW, and the switching frequency 50kHz is for safety. Electrical isolation between high and low voltage terminals is necessary. Then, the low voltage terminal of high-frequency transformer is referred to as the earth. With respect to the low pressure end, the high end ground state is suspended. The system is composed of two full bridge connected by high-frequency transformer. In boost mode, the M1-M4 signal is controlled by PWM signal with duty ratio greater than 0.5, which is phase shifted compared with M2-M3 controller. 180 the leakage inductance of the transformer usually produces high voltage pulses on the main power devices, and the circuit loads of MCL DCL and CCL are responsible for the suppression of these pulses. The electric power stored in the clamping process of the clamp capacitor CCL is introduced into the main power circuit, which saves a large amount of electric energy than the traditional consumable buffer. In the depressurization mode, the converter uses a phase-shift modulation method to control the high pressure bridge arm by this way. According to transformer leakage inductance and output capacitance of the device, zero voltage switching operation (ZVS) is implemented in load range. Two direction PWM signals must be properly controlled, so that the converter can achieve maximum energy efficiency. To achieve the best current charging curve and improve the energy efficiency of the battery, there are three current sensors and two voltage sensors in the DC to DC converter control structure. Figure 4 shows the control system of the circuits.The add-edge-rule is designed base on the local consistency score criterion in the new algorithm. And the rule is embedded in the framework of ant colony algorithm. Therefore, the new algorithm can use the heuristic to dynamically reduce the search space and reduce the running time during the search process. The empirical tests show that without loss of results accuracy, the convergence speed of the proposed algorithm is significantly 40% faster than that of ant colony optimization. In addition, the Bayesian classifier based on constrained ant colony algorithm is proposed for project's risk prediction of real estate project in the stage of decision. The basic equation is shown below:

$$E_p f_i = \sum_{x,y} \overline{p}(x)\, p(y/x)\, f_i(x,y) \tag{1}$$

$\bar{p}(x)$ represents experience marginal distribution of x in the training sample. The expectation value calculated by model should be consistent with experience expectation value.

$$C = \{p / E_p f_i = E_{\bar{p}} f_i, i \in \{1,2,...,K\}\} \tag{2}$$

C represents a series of probability distribution. The core idea of maximum entropy is to choose the model with largest entropy in these models. In all probability distribution, *p** is selected, which meets the following equation.

$$H(p) = -\sum_{x,y} \bar{p}(x) p(y/x) \log p(y/x) \quad p^* = \arg\max_{p \in C} H(p) \tag{3}$$

H(*p*) represents condition entropy used to represent evenness of condition probability *p*(*y*|*x*). This is an optimization problem; the introduction of Lagrange operator makes us get the form of solution.

$$p^*(y/x) = \frac{1}{Z(x)} \exp\left(\sum_{i=1}^{K} \lambda_i f_i(x,y)\right) \quad Z(x) = \sum_x \exp\left(\sum_{i=1}^{K} \lambda_i f_i(x,y)\right) \tag{4}$$

In the above formula

$$A_{mn} + jB_{mn} = \frac{2}{(2\pi)^2} \int_{-\pi}^{\pi} \int_{-\pi}^{\pi} u_{P1}(X,Y) e^{j(mX+nY)} dXdY \tag{5}$$

Take the formula (2) into formula (3)

$$\begin{aligned} A_{mn} + jB_{mn} &= \frac{E}{6\pi^2} \int_0^{\pi} \int_{2\pi k+\pi-\alpha_1-\pi M \sin Y}^{2\pi k+\pi-\alpha_1+\pi M \sin Y} e^{j(mX+nY)} dXdY \\ &= \frac{E}{j6m\pi} e^{jm(n-\alpha_1)} [\frac{1}{\pi} \int_0^{\pi} e^{jmM\pi \sin Y} e^{jnY} dY - \\ &\frac{1}{\pi} \int_0^{\pi} e^{-jmM\pi \sin Y} e^{jnY} dY] \end{aligned} \tag{6}$$

By Bessel function, we have:

$$L = \min\left(\sum_{k=1}^{n} d(k-1,k) + d(n,0)\right) \tag{7}$$

Based on the gradient descent method, node center and base width parameter are:

$$\begin{aligned} &w_j(k) = w_j(k-1) + \eta(y(k) - y_m(k)) h_j \quad \Delta b_j = (y(k) - y_m(k)) w_j h_j \left(\frac{\|X - C_j\|^2}{b_j^3}\right) \quad b_j(k) = b_j(k-1) + \eta \Delta b_j \\ &+\alpha(w_j(k-1) - w_j(k-2)) \qquad\qquad +\alpha(b_j(k-1) - b_j(k-2)) \end{aligned} \tag{8}$$

Two voltage sensors are used to adjust the voltage of the two battery, and two current sensor for current control of two battery charging curve, third current sensors are used to control the current transformer saturation, prevent power devices damaged in the explanation of these two control strategies, we should distinguish the charging process of the following: (1) high pressure the battery is responsible for maintenance of the battery charging; (2) the maintenance of the battery to charge the battery for high pressure. In the maintenance process of charging the battery, DC - DC converter in Buck mode, the voltage from 400 V to 12 V, the low end switch does not work, only to achieve a continued flow diode rectifier voltage level of its built-in, four switch and PWM signal drive high voltage side of the selected control strategy for phase modulation method. Two fixed duty cycle of 50% complementary signals driving two switch on each arm, and between the two bridge arm signal phase angle by the control network determines the control strategy to prevent the use of symmetrical transformer core saturation adjustment, and buck converter duty cycle control, maintenance of battery charging by setting the dead time suitable for driving two of full bridge inverter complementary devices, the MOSFET is exactly zero voltage turn-on, so as to eliminate the conduction loss problem. As shown in

Figure 5, when the M5 is turned from a pilot to a turn off, the M7 is still closed because of the dead time, and the center point of the half bridge will be suspended.

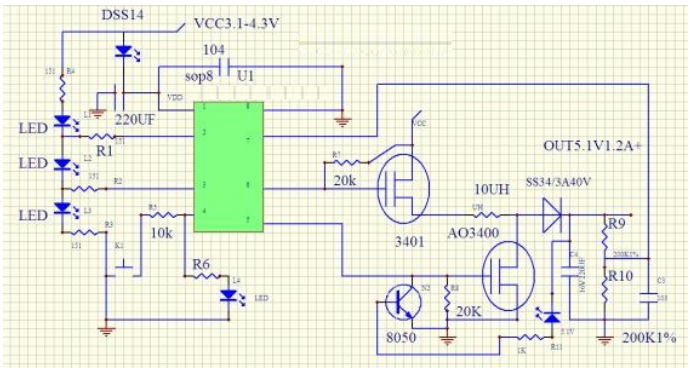

Figure 4: The DC/DC converter control circuit

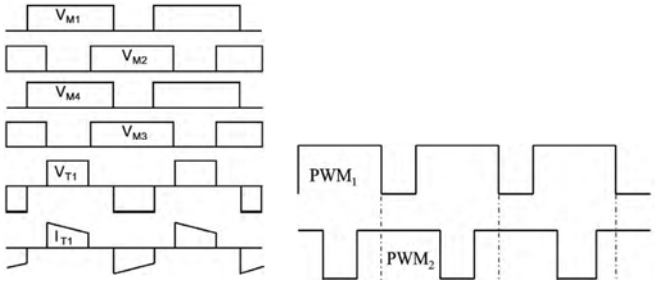

Figure 5: PWM control

Moreover, because the resonant circuit consisting of transformer leakage inductance and parasitic capacitance is located at the center point of the half bridge, it will generate natural oscillation, which will cause VDS6 to oscillate at fixed frequency. By setting the dead time correctly, M6 can be judged at zero voltage. Finally, in order to further improve the energy efficiency of the converter, M2-3 and M1-4 are driven by AND signals of the PWM signals of the high voltage terminals to achieve synchronous rectification function, so as to reduce the pressure drop when the freewheeling diodes are on the way. When charging the high pressure battery, the DC - DC converter sends electrical energy back to the high voltage battery group and increases the voltage from 12V to 400V. At this time, the high voltage end full bridge switch does not work, and the continuous current diode only performs the voltage rectifying function. At the low voltage end, the full bridge switch must be properly controlled to perform the boost operation and reduce the power loss to the maximum. The bootstrap circuit operation is implemented by a very convenient strategy: a two duty cycle PWM signal is higher than 50% to drive the two diagonal switch 180 degrees phase angle, this method allowing for an overlap period, all four switches are closed at the same time to charge the input inductor. At the same time, through the parallel two MOSFET bridge arms, the maximum resistance RD-Son is reduced to the maximum. In the remaining two cycles, another diagonal switch is directed, allowing the power to pass through the magnetic transformer by using the first and third quadrants. STM32F103 RC is the focus of the development of this application design, because the micro controller embedded with a powerful set of motor control peripherals, to allow very low CPU load to the system (double H bridge) to provide the correct vector of the core application design is the use of cross triggering unit (CTU) and eDMA (enhanced direct memory access), allowing users to trigger all the ADC capture and PWM configuration, without any CPU intervention in this case, a high degree of integration of motor control peripherals group (CTU-FlexPWM-ADC-DMA) that CPU performs control algorithm based on plant variables, namely the implementation of the control algorithm in each control period of 20 microseconds. Will CPU the actual occupancy rate decreased below 35%, such as the release of more performance to perform other tasks, and system security measures more (i.e. PWM generated /IO Redundant control) CTU activity is synchronized with the PWM cycle of the application, based on a pre-programmed list of instructions (two ADC units) that trigger automatic ADC acquisition.
ADC CTU ADC are all collected in FIFO, once the value reaches a preprogrammed threshold, immediately trigger to transfer operation from SRAM DMA once and then the data pretreated by CPU (because the

induction variable sampling completed) sent to the control algorithm, PWM control algorithm for vector control algorithm for fixed point the next control cycle, each direction conversion by two PID controller. Two ADC modules are implemented on the device. Each module contains user configurable sampling rate and conversion times. In this application, the total time of sampling and collecting data from the channel is less than 0.9 microseconds. The divider generates the ADC clock signal through the clock of the ADC digital interface. The internal simulation dog of ADC will compare the value of the converted data with the user programming threshold. If the converted data exceeds the threshold, an interrupt signal will be generated. Each ADC is controlled by the CPU (CPU control mode) and the CTU (CTU control mode). CTU can use an ADC command to control ADC sampling, but the premise is that ADC is in the CTU control mode. In this case, two ADC acquisition operations can be triggered at the same time. In this application, two ADC collects three current values and two voltage values, and converts them to 10 bit resolution data (maximum voltage 3.3V). Figure 6 shows the result.

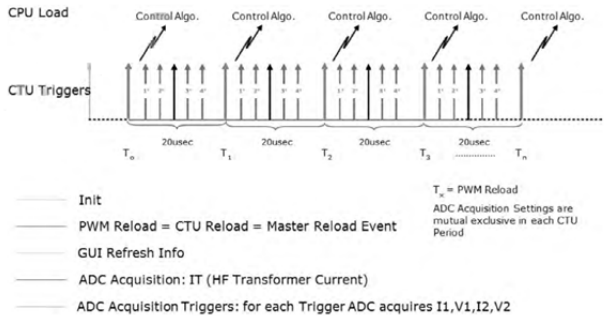

Figure 6: The control result

4. Conclusion

The cycle of PWM signal involved in this application is 20 microseconds (DC to DC switching frequency 50 kHz), so select sub module 0 to synchronize / reload all PWM sub modules, so as to avoid losing match between PWM signals. The same module is also used to restart the CTU control cycle. Phase modulation (HV H bridge) PWM signal is 0 and 1 sub modules, each module produces two signals, each signal (in the same sub module) are complementary (only different dead time). The sub module 1 has a delay between the generated signal of the sub module 0, and the delay time is a phase-shift modulation value generated by the DC/DC control algorithm. The synchronous rectifier is based on the two signals generated by the sub module 2. Duty ratio modulation based on sub module 2 signal (like phase modulation synchronous rectifier one) sample. The signal duty ratio varies in the range of [52%, 90%], and the second signal is delayed by half a period (10 microseconds). The sub module 3 provides a dual switch output signal to generate the required active clamp PWM signal.

References

Baloch M.H., Wang J., Kaloi G.S., 2016, Stability and nonlinear controller analysis of wind energy conversion system with random wind speed, International Journal of Electrical Power & Energy Systems, 79(11), 75-83, DOI: 10.1016/j.ijepes.2016.01.018.

Cárdenas R., Díaz M., Rojas F., Clare J., 2016, Resonant control system for low-voltage ride-through in wind energy conversion systems, IET Power Electronics, 9(6), 1297-1305, DOI: 10.1049/iet-pel.2015.0488.

Errami Y., Ouassaid M., Maaroufi M., 2015, A performance comparison of a nonlinear and a linear control for grid connected PMSG wind energy conversion system. International Journal of Electrical Power & Energy Systems, 68, 180-194, DOI: 10.1016/j.ijepes.2014.12.027.

Sun L., Zhang N., 2015, Design, implementation and characterization of a novel bi-directional energy conversion system on DC motor drive using super-capacitors, Applied Energy, 153, 101-111, DOI: 10.1016/j.apenergy.2014.06.084.

Tanvir A.A., Merabet A., Beguenane R., 2015, Real-Time Control of Active and Reactive Power for Doubly Fed Induction Generator (DFIG)-Based Wind Energy Conversion System, Energies, 2015(8), 10389-10408, DOI: 10.3390/en80910389.

Yang Y., Mok, K.T., Tan, S.C., Hui, S.Y., 2015, Nonlinear Dynamic Power Tracking of Low-Power Wind Energy Conversion System, IEEE Transactions on Power Electronics, 2015, 30(9), 5223-5236, DOI: 10.1109/TPEL.2014.2363561.